

Supplemental information

Figure S1. The temperature correction applied to the *in situ* experiments used the regression equations for above and below room temperature.

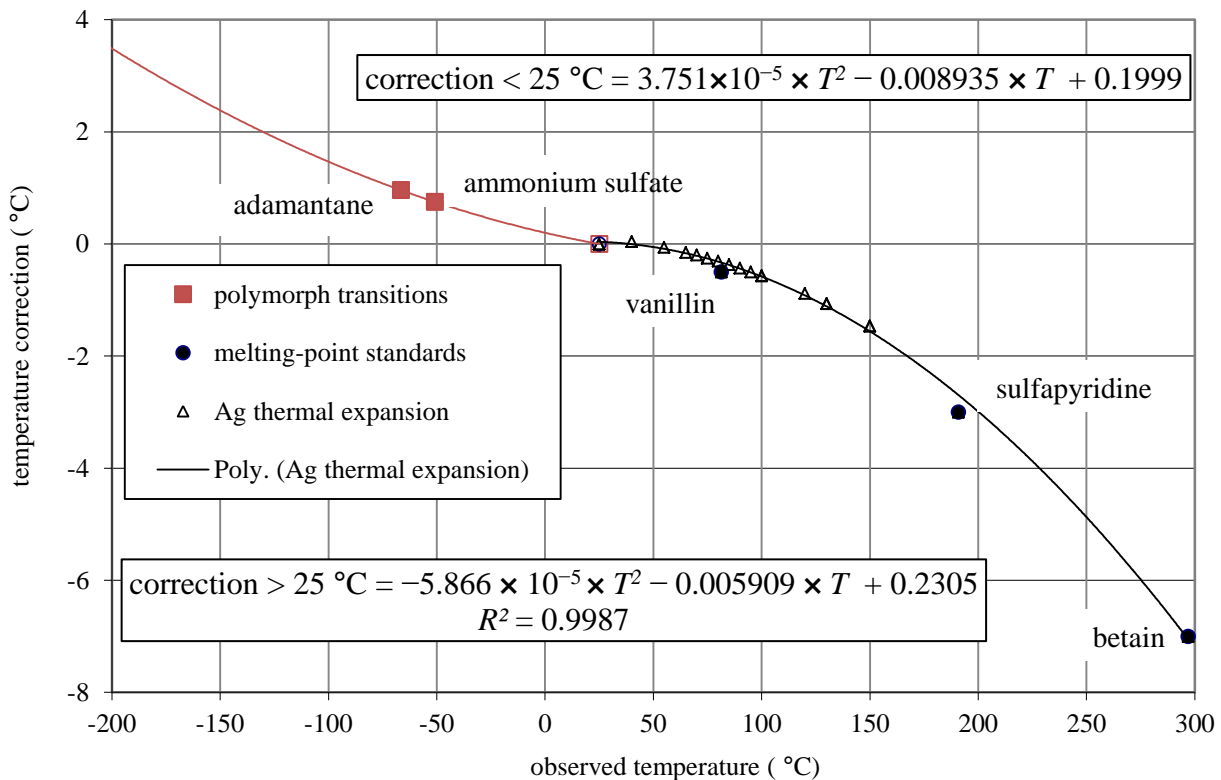


Figure S2. XRPD patterns of the ammonium sulfate 200 *hkl* near the polymorphic transition at $-50.0\text{ }^{\circ}\text{C}$ were used for correcting the *in situ* low-temperature experiments.

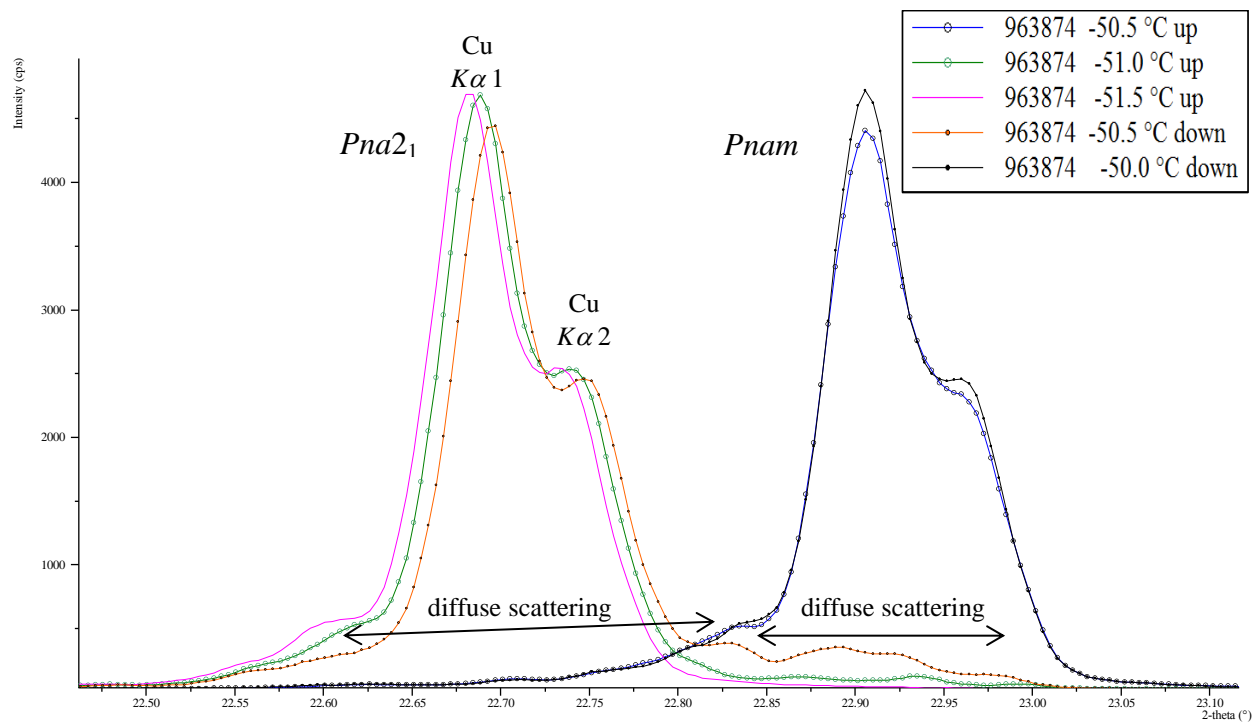
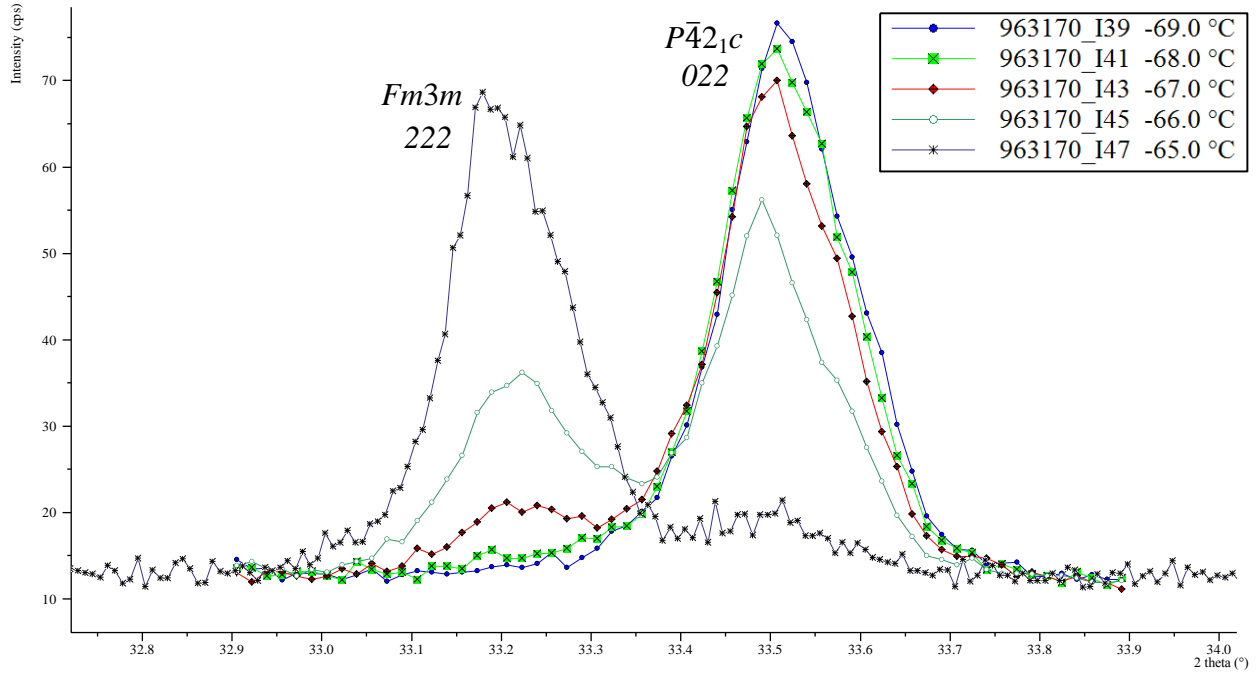


Figure S3. XPRD patterns of adamantane near the face-centered to primitive polymorphic transformation at $-65.5\text{ }^{\circ}\text{C}$ were used for correcting the *in situ* low-temperature experiments.



$Fm\bar{3}m$ $a = 9.341\text{ \AA}$ at $-64.0\text{ }^{\circ}\text{C}$

$P\bar{4}2_1c$ $a = 9.341\text{ \AA}$ and $c = 8.964\text{ \AA}$ at $-67.0\text{ }^{\circ}\text{C}$

Figure S4. Fraction of ccp adamantane as a function of temperature near the transformation at $-65.5\text{ }^{\circ}\text{C}$ (bold vertical line). The correction temperature (X) is at the 0.5 fractional amount.

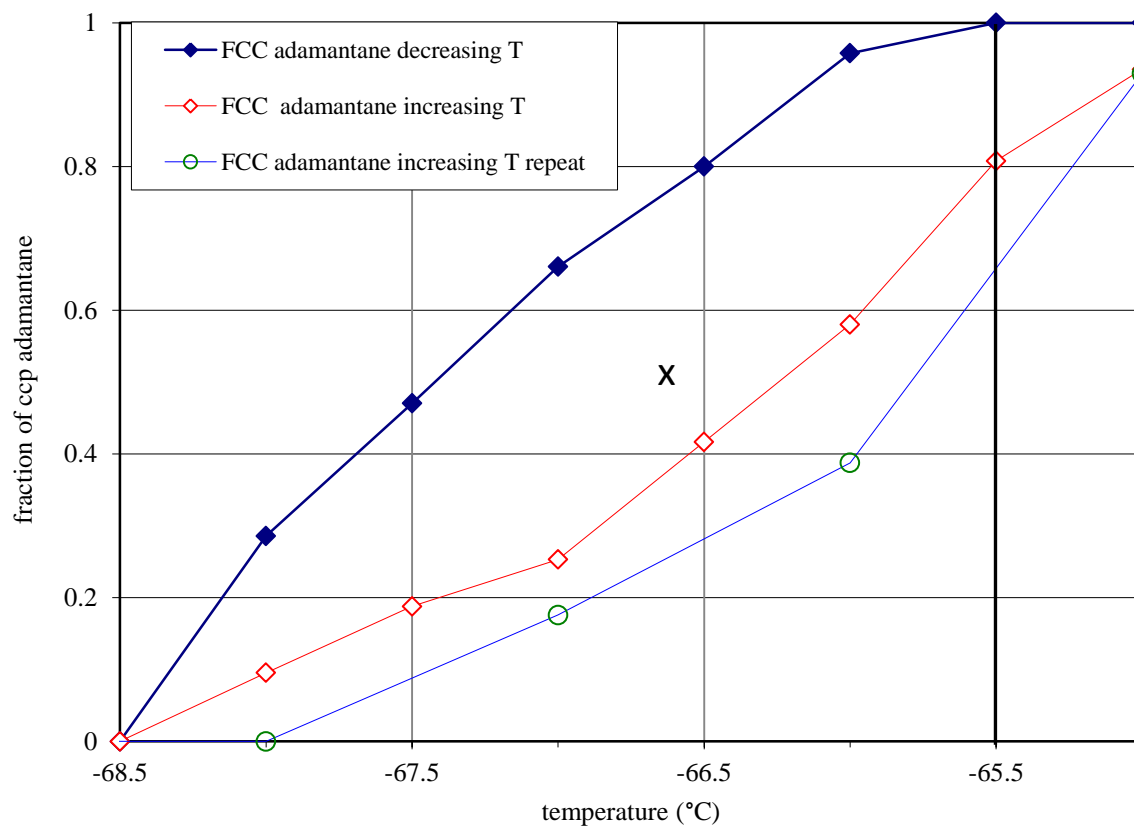


Figure S5. The thermal reaction of film 1 ramped to 130 °C Ag_3O at 35 °C/min and scanned for 41 h.

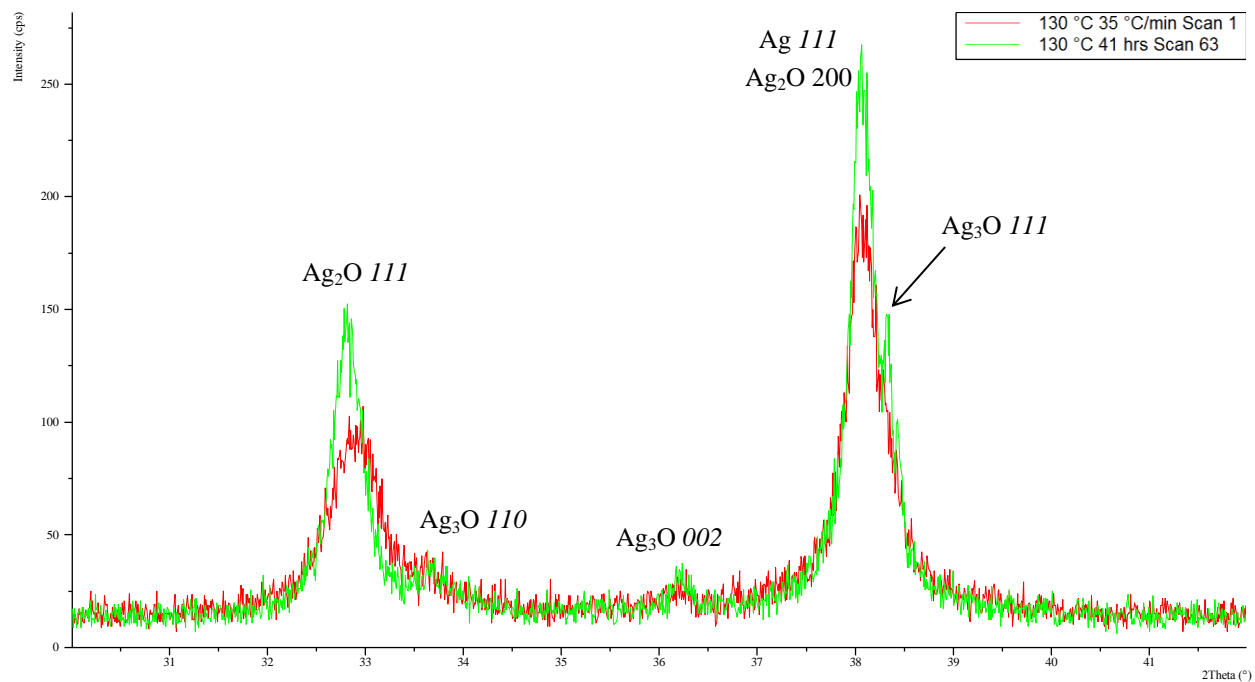


Figure S6. The Ag_3O wt. % versus unit-cell volume at ambient conditions for the *ex situ* products of ball-milled jet-milled film (B1).

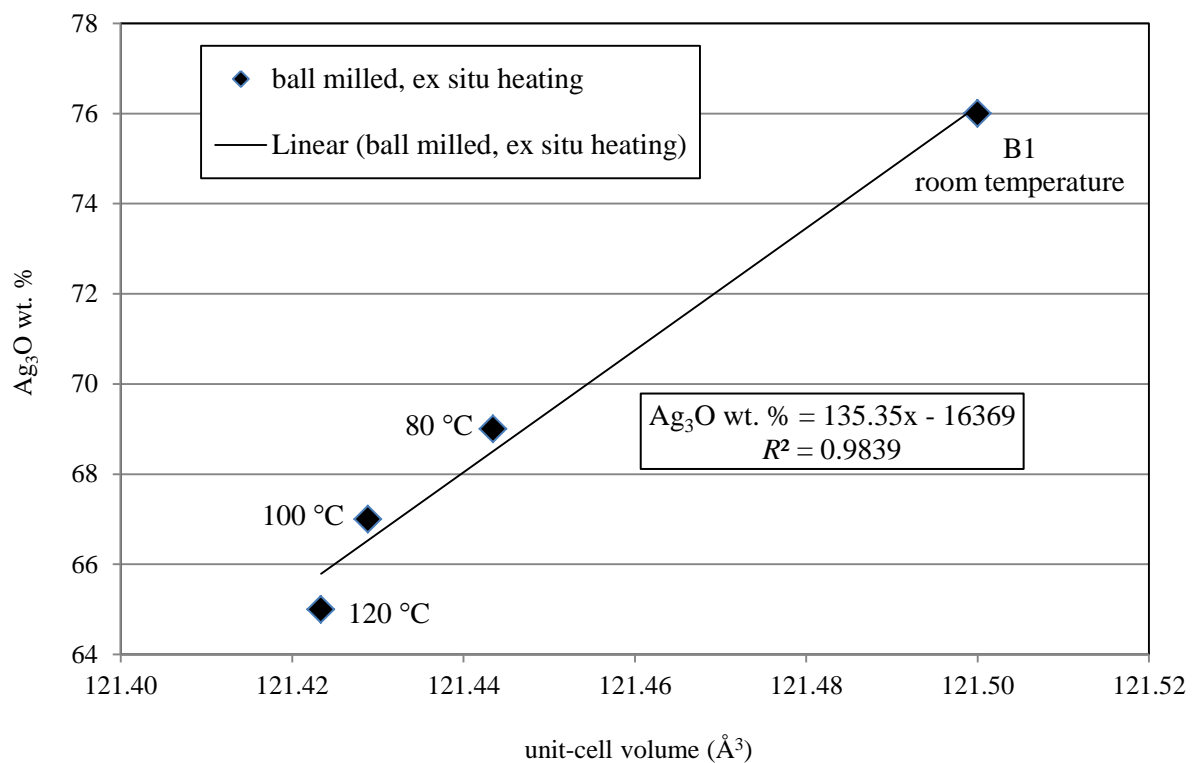


Figure S7. The Ag_3O a axis and c axis at ambient conditions for the *ex situ* products of reacted jet-milled films. The data from Beesk *et al.* (1981) (grey square) were measured on a single crystal hydrothermally synthesized on Ag metal and were scaled using Mo $K\alpha$ from TOPAS as shown by the arrow from the grey square to the black square.

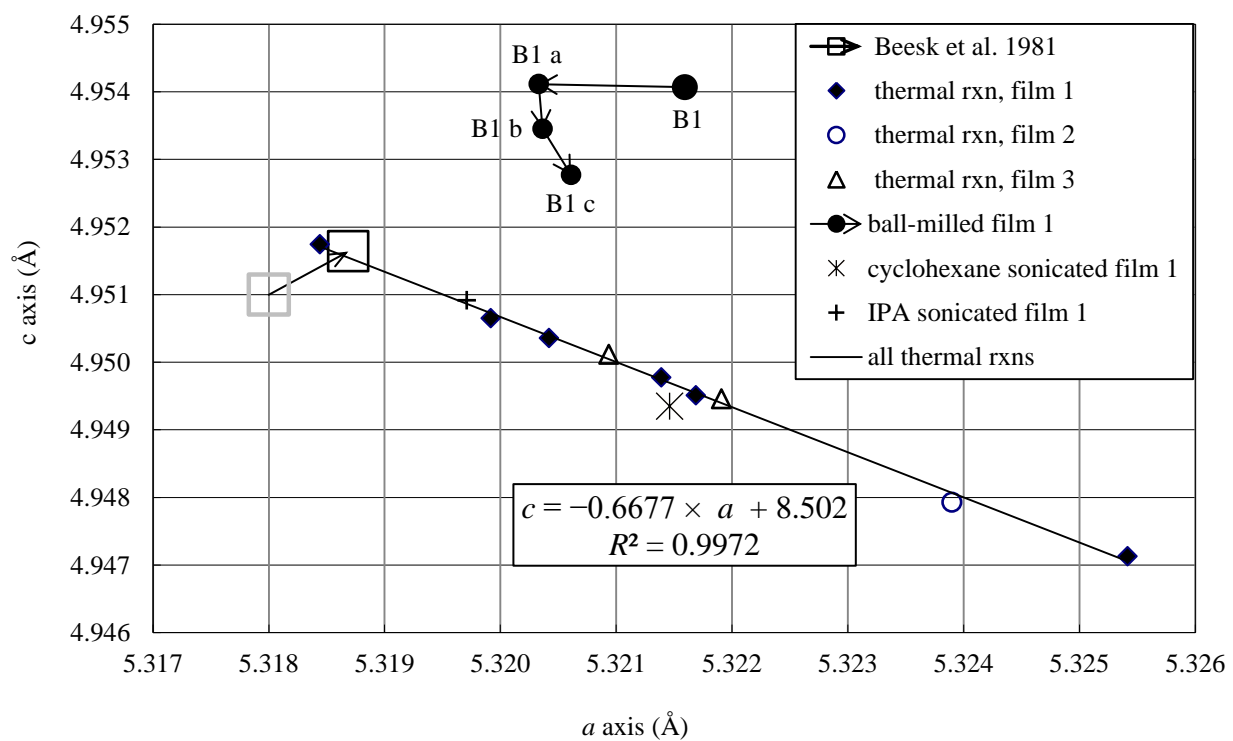
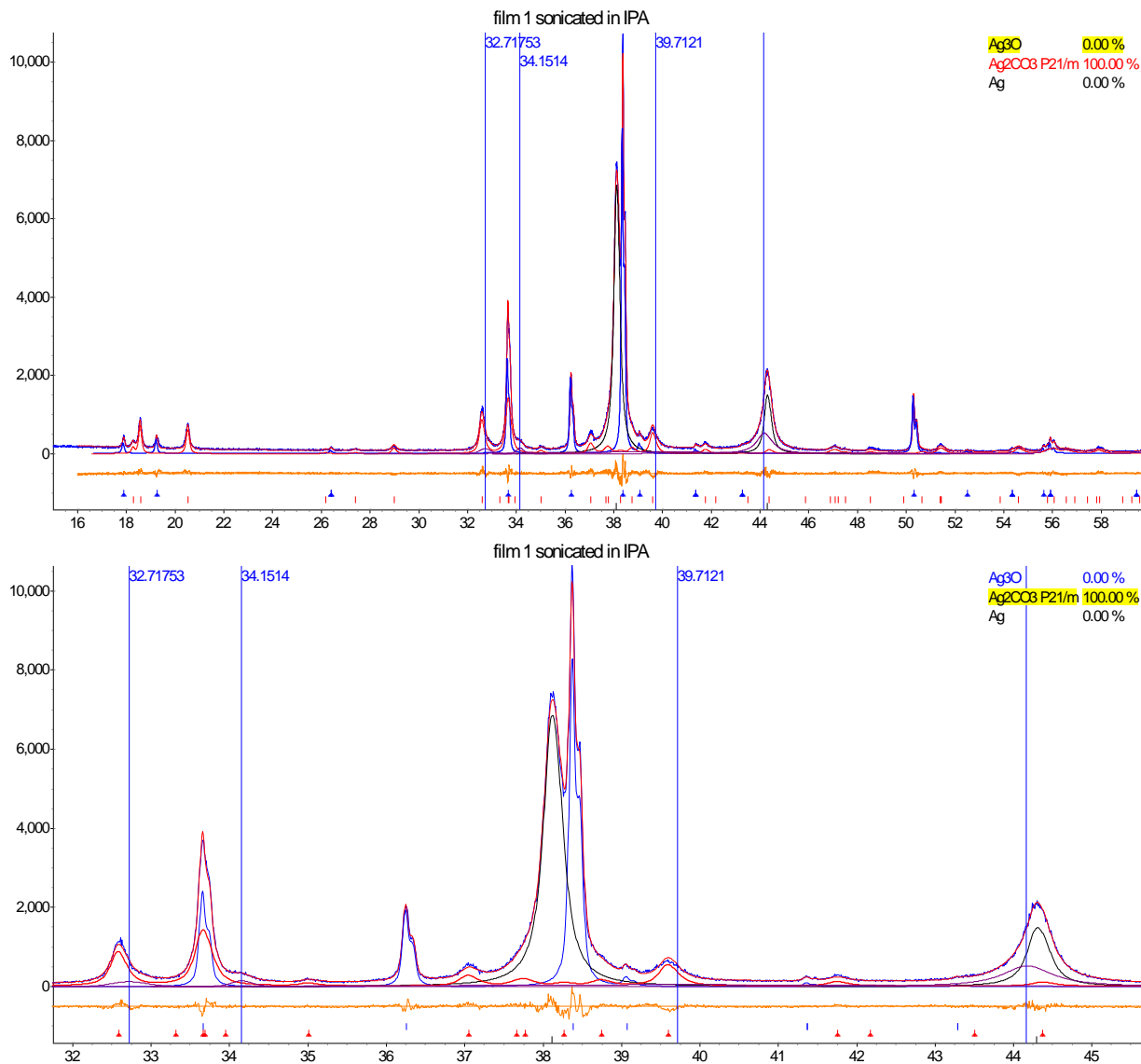
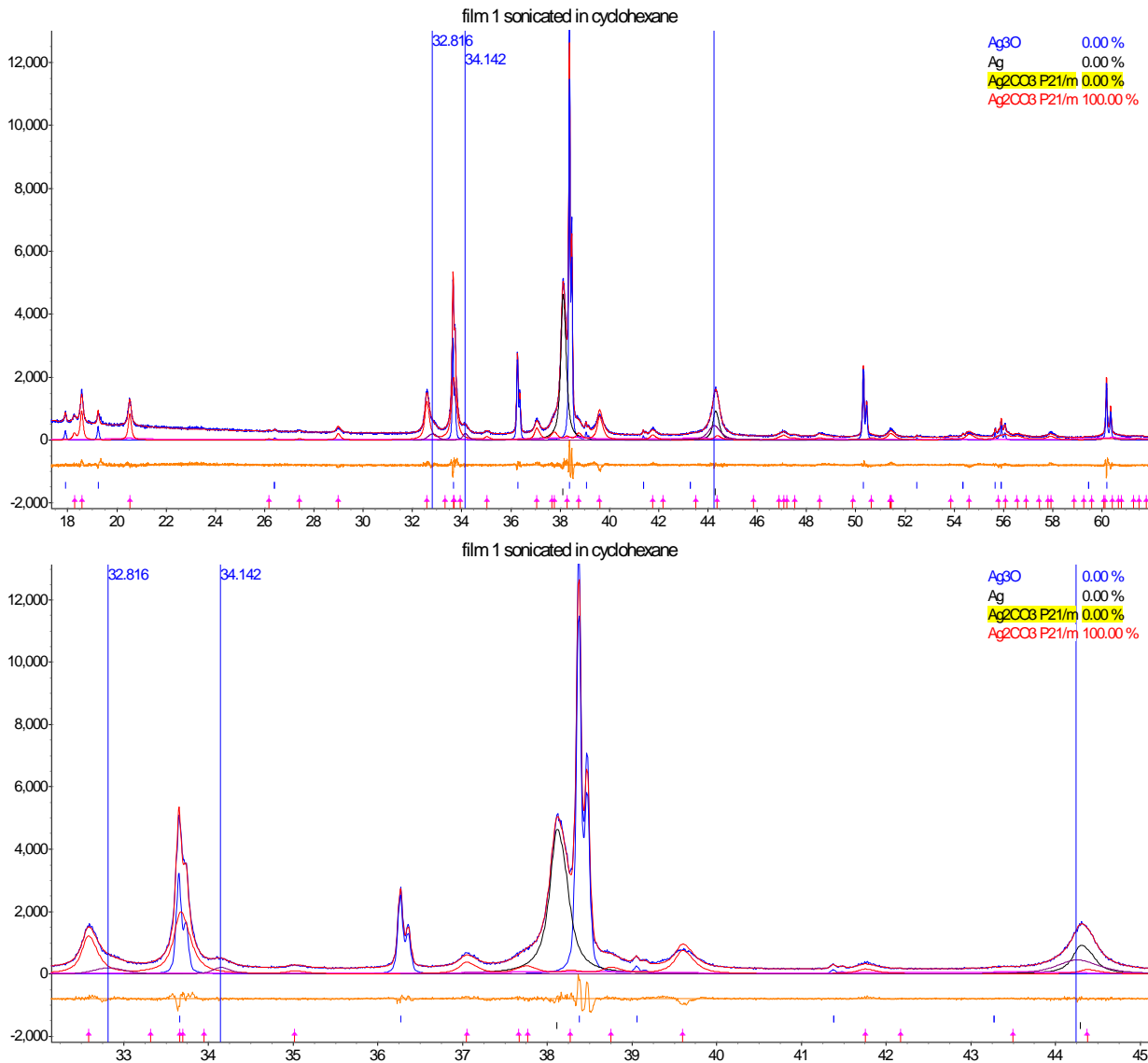


Figure S8. The refinement for film 1 sonicated in isopropyl alcohol for 45 sec using a TOPAS “structure” model for refining LT Ag_2CO_3 . The peak at 32.718° overlaps the peak for $\text{Ag}_2\text{O III}$, the intensity at 32.72° and 34.15° is likely generated by stacking faults in Ag_3O and/or disordered $\beta \text{Ag}_2\text{CO}_3$, and the intensity near 44.2° is from LT Ag_2CO_3 and stacking faults in Ag.



$P2_1/m$				
$a = 4.85205 \text{ \AA}$				
$b = 9.54498 \text{ \AA}$				
$c = 3.25386 \text{ \AA}$				
$\beta = 92.02^\circ$ cell volume $150.60(2) \text{ \AA}^3$				
linear-absorption coefficient = 1023.24 cm^{-1} density = 5.817 g/cm^3				
GOF	R_{exp}	R_{wp}	R_p	Weighted Durbin Watson
1.53	5.66	8.66	6.01	1.04
2 θ zero offset = 0 fixed			sample displacement = 13 μm	

Figure S9. The refinement of film 1 sonicated in cyclohexane for 3 min using a TOPAS “structure” model for refining LT Ag_2CO_3 . The intensity at 32.816° is part of the Ag_2O 111 , the intensity at 34.142° is likely generated by stacking faults in Ag_3O and/or disordered β Ag_2CO_3 , and the intensity near 44.2° is from stacking faults in Ag and from LT Ag_2CO_3 .



$P2_1/m$				
$a = 4.85242 \text{ \AA}$				
$b = 9.54529 \text{ \AA}$				
$c = 3.25369 \text{ \AA}$				
$\beta = 92.02^\circ$ cell volume = $150.61(2) \text{ \AA}^3$				
linear-absorption coefficient = 1023.19 cm^{-1} density = 5.817 g/cm^3				
GOF	R_{exp}	R_{wp}	R_p	weighted Durbin Watson
1.66	4.96	8.25	5.95	0.84
2 θ zero offset = 0 fixed			sample displacement = -3 \mu m	

Ag_3O ms12

Figure S10. The FWHM(T) of the diffuse peak at $\sim 33.6^\circ$ for the *in situ* thermal reaction of film 1 and reaction products 1d and 3b.

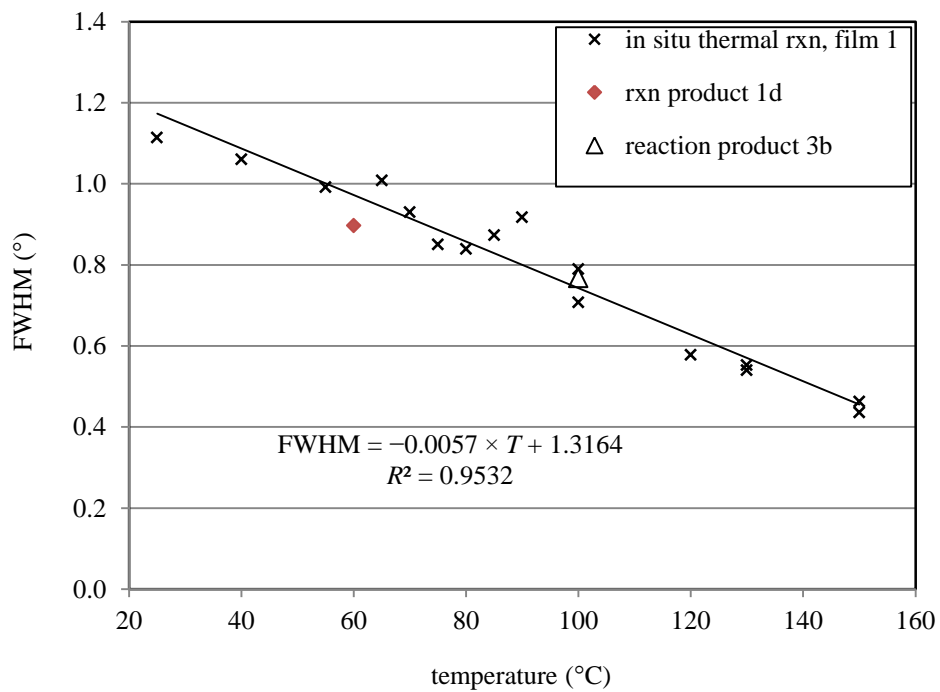
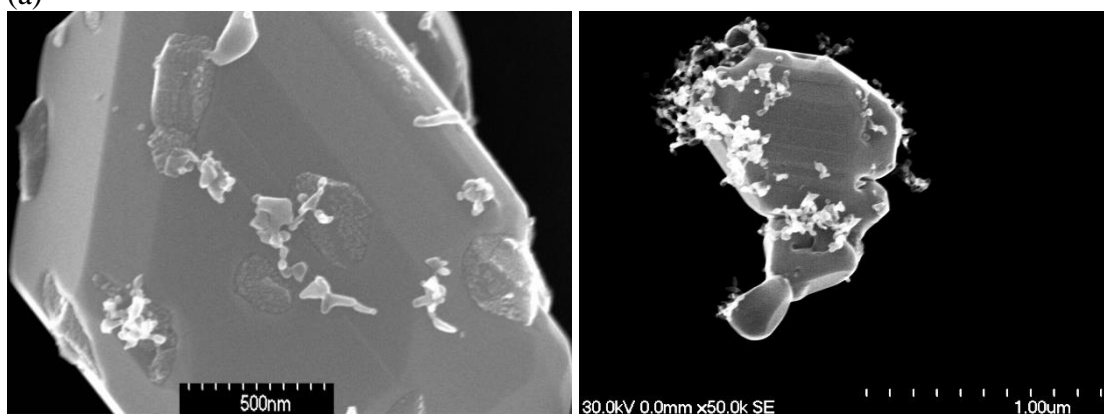
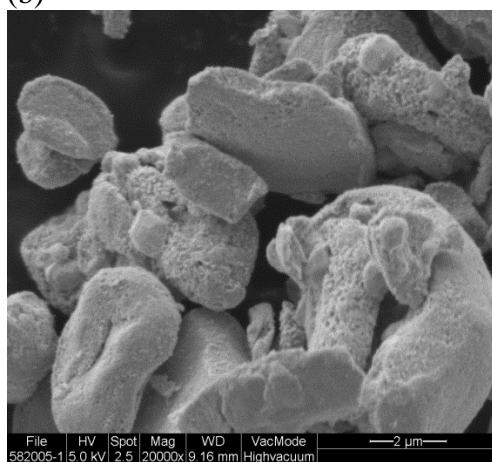


Figure S11. SEM photomicrograph of (a) faceted Ag_3O crystals produced by a thermal reaction of a jet-milled thin film; temperature and time period unavailable, (b) the product from the *in situ* thermal reaction of film 1 after 148 °C and 39 h (III.B), and (c) *ex situ* thermal-reaction product 1e (60 °C, 1 yr).

(a)



(b)



(c)

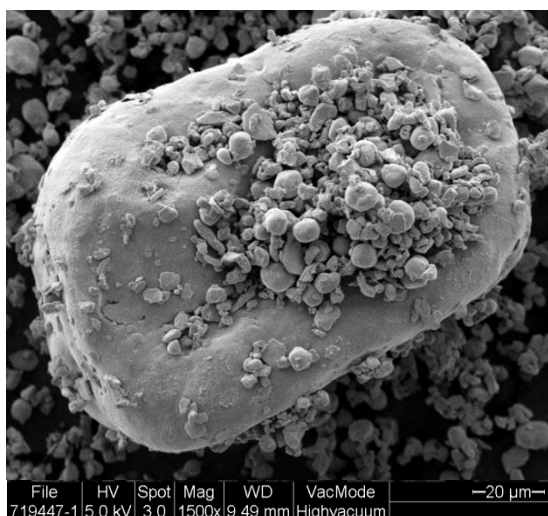


Figure S12. Published Ag_2O $a(T)$. The *ex situ* values at ambient T from Allen (1960), Favre (1940), and Taylor *et al.* (2005) were corrected for thermal expansion and graphed at their annealing temperatures.

